Monthly Notices of the ROYAL ASTRONOMICAL SOCIETY

MNRAS **468,** 3212–3222 (2017) doi:10.1093/mnras/stx552
Advance Access publication 2017 March 8

Particle tagging and its implications for stellar population dynamics

Theo Le Bret,[1,2⋆] Andrew Pontzen,[1] Andrew P. Cooper,[3] Carlos Frenk,[3] Adi Zolotov,[4] Alyson M. Brooks,[5] Fabio Governato[6] and Owen H. Parry[7]

[1]*University College London, London WC1E 6BT, UK*
[2]*Rudolf Peierls Centre for Theoretical Physics, University of Oxford, Oxford OX1 3NP, UK*
[3]*Institute for Computational Cosmology, Durham University, South Road, Durham DH1 3LE, UK*
[4]*Department of Physics, Center for Cosmology and Astroparticle Physics, The Ohio State University, OH 43210, USA*
[5]*Rutgers, the State University of New Jersey, Department of Physics & Astronomy, 136 Frelinghuysen Rd, Piscataway, NJ 08854, USA*
[6]*Astronomy Department, University of Washington, Box 351580, Seattle, WA 98195-1580, USA*
[7]*Department of Astronomy, University of Maryland, College Park, MD 20742, USA*

Accepted 2017 March 1. Received 2017 March 1; in original form 2015 January 26

ABSTRACT

We establish a controlled comparison between the properties of galactic stellar haloes obtained with hydrodynamical simulations and with 'particle tagging'. Tagging is a fast way to obtain stellar population dynamics: instead of tracking gas and star formation, it 'paints' stars directly on to a suitably defined subset of dark matter particles in a collisionless, dark-matter-only simulation. Our study shows that 'live' particle tagging schemes, where stellar masses are painted on to the dark matter particles dynamically throughout the simulation, can generate good fits to the hydrodynamical stellar density profiles of a central Milky Way-like galaxy and its most prominent substructure. Energy diffusion processes are crucial to reshaping the distribution of stars in infalling spheroidal systems and hence the final stellar halo. We conclude that the success of any particular tagging scheme hinges on this diffusion being taken into account, and discuss the role of different subgrid feedback prescriptions in driving this diffusion.

Key words: methods: numerical – galaxies: formation – galaxies: haloes – galaxies: structure.

1 INTRODUCTION

Observations of the stellar halo around Local Group galaxies provide strong constraints on different models of galaxy formation (for historical context see, for instance, Eggen, Lynden-Bell & Sandage 1962; Searle & Zinn 1978). In today's standard Λ cold dark matter (CDM) cosmology, large galaxies such as the Milky Way (MW) are predicted to form in part through the progressive mergers of smaller progenitor galaxies (White & Rees 1978; Frenk et al. 1985; White & Frenk 1991; Kauffmann, White & Guiderdoni 1993), and the observed stellar halo is formed, in one way or another, from the remnants of this hierarchical assembly (Helmi & White 1999; Helmi et al. 1999; Abadi, Navarro & Steinmetz 2006).

While the current consensus is that the stellar halo forms primarily via accretion of stars from tidally stripped satellites (e.g. Bell et al. 2008), there remain a number of open questions: for instance, does the halo form exclusively from accretion, or are some halo stars formed within the main galaxy (referred to as in situ stars) during dissipative collapse? Are further stars kicked up from the disc to form an important fraction of the halo (Zolotov et al. 2009, 2010; Font et al. 2011; Tissera et al. 2013)? Do the main progenitors of the stellar halo survive as satellite galaxies to the present day (Cooper et al. 2010) or are they mostly fully disrupted (Bullock & Johnston 2005)?

In principle, cosmological simulations of galaxy formation that self-consistently follow the evolution of a baryonic component can be used to predict the properties of galactic haloes and provide answers to these questions. In practice, however, this is challenging because large particle numbers are required to resolve any detail within the faint, diffuse stellar halo, which contains only a few percent of all the stars in the galaxy. Only recently has it become possible to start studying some halo properties in this self-consistent way (e.g. Zolotov et al. 2009).

As an alternative, some authors have proposed using dark-matter-only (DMO) *N*-body simulations – which are significantly less computationally expensive than hydrodynamical simulations – where stellar populations are 'painted' on to dark matter (DM) particles to reproduce the collisionless assembly of the stellar halo (Bullock & Johnston 2005; De Lucia & Helmi 2008; Cooper et al. 2010; Rashkov et al. 2012; Laporte, Walker & Peñarrubia 2013). Such methods have been used to make quantitative predictions of halo substructure and dynamics (Cooper et al. 2011, 2013; Helmi et al. 2011; Gómez et al. 2013), but the validity of the

⋆ E-mail: theo.lebret@astro.ox.ac.uk

assumptions underpinning these DMO models remains controversial (e.g. Bailin et al. 2014).

So at present there are two techniques – hydrodynamic simulations and particle tagging – for investigating stellar halo structure that have their own strengths and weaknesses. Recent work has demonstrated that significant discrepancies between the two approaches can arise (Bailin et al. 2014). In this paper, we will investigate a specific tagging scheme (that of Cooper et al. 2010) and by comparing its predictions to those of hydrodynamical simulations, aim to understand better how and why differences between predictions arise. While this does not immediately resolve the question of how to produce 'correct' predictions for the stellar halo, it does give a physical basis for understanding discrepancies and so highlights some essential prerequisites for realistic modelling.

This paper is structured as follows. In Section 2, we provide an overview of the tagging technique, stating its main assumptions; in Section 3, we describe the simulations used in our study, and how they are used to establish a controlled comparison between tagging and smoothed particle hydrodynamics (SPH); in Section 4, we present the outcome of the simulations, and compare the structure of the different stellar haloes obtained; in Section 5, we discuss the role of diffusion processes in shaping realistic tagged haloes, and give a new interpretation for the model-to-model discrepancies found in the literature; in an appendix, we further show that this behaviour is generic. Finally, in Section 6, we explain the overall physical picture that emerges and highlight how this should affect the future direction of tagging and broader investigations of the stellar halo.

2 PARTICLE TAGGING

Various methods have been proposed for associating a stellar component with particles from DMO simulations (Bullock & Johnston 2005; Cooper et al. 2010; Libeskind et al. 2011; Rashkov et al. 2012; Bailin et al. 2014). DM particles that are tightly bound to their haloes are assigned 'stellar masses' according to an assumed star formation rate (SFR), and the evolution of these painted particles is then traced up to $z = 0$, where their final distribution is taken to represent the distribution of stars in the real stellar halo.

These methods rely on three assumptions.

(i) Stars form tightly bound to their parent haloes (e.g. with binding energies typically larger than 90–99 per cent of the DM particles), with energy distributions similar to those of the 'most-bound' fraction of DM particles.

(ii) Recently formed star particles and their tagged DM analogues subsequently follow similar phase space trajectories. In other words, selecting the correct initial binding energy for the tagged DM particles is assumed to be sufficient to ensure the correct subsequent kinematics. This assumption could fail given that, for instance, DM particles and stars with similar binding energy will not necessarily have similar angular momentum.

(iii) Baryonic effects are not important in shaping the stellar halo. For instance, the coupling between the dynamics of DM and baryons due to supernova (SN) feedback (Pontzen & Governato 2014) cannot be modelled by tagging a DMO simulation, and so is simply assumed to be unimportant for the dynamics of halo stars; the final distribution of stars in the halo is taken to be governed purely by the dynamics of accretion, and insensitive to the detailed baryonic processes that take place where these and subsequent generations of stars formed.

The first assumption is not likely to be problematic, as stars will tend to form fairly deep in their host DM halo's potential well. However, the second assumption raises two separate concerns: first, that stars kicked up from the disc of the central galaxy may contribute an 'in situ' component to the stellar halo (see for instance; Zolotov et al. 2009; Font et al. 2011), which by definition cannot be represented in a DMO simulation; secondly, stars that form in the discs of satellites and are subsequently accreted by the central galaxy will have different kinematics from their tagged DM analogues. The first issue is dealt simply by stating that tagging schemes will only consider the accreted part of the halo, and neglect any in situ contribution. Addressing the second issue requires an explicit comparison between the satellite stellar density profiles produced by tagging and methods that include baryons, which is one of the aims of this paper. Finally, the last assumption (unimportance of baryons) can affect the validity of tagging in two ways: first, the presence of a baryonic disc potential can cause real haloes to be less prolate than the tagged DM haloes (Bailin et al. 2014), thus adding a caveat to the interpretation of tagging schemes – though an analytic potential can be added to the DMO simulation to alleviate this, as in Bullock & Johnston (2005); secondly, baryonic feedback in real satellites can affect the orbits of both the stellar and DM component through dynamical core creation (Navarro, Eke & Frenk 1996; Read & Gilmore 2005; Maxwell et al. 2012; Pontzen & Governato 2012), which in turn may increase the likelihood of these satellites being tidally disrupted (Peñarrubia et al. 2010; Parry et al. 2012; Zolotov et al. 2012), and thus be significant in shaping the stellar halo properties.

The specific tagging scheme we investigate in this paper is described by Cooper et al. (2010), hereafter C10, where a fixed most-bound fraction ($f_{\rm mb}$, usually chosen to lie between 1 and 10 per cent) of DM particles in each halo are tagged at every simulation output time, being assigned 'stellar masses' (as well as ages and metallicities) according to the prescriptions of a semi-analytic model of galaxy formation, GALFORM (see Cole et al. 2000 for details and Baugh 2006 for an overview of hierarchical galaxy formation with semi-analytic models).

We will briefly discuss the relevance of our conclusions to tagging schemes that paint the DM particles at the time of satellite infall (Bullock & Johnston 2005; Libeskind et al. 2011) in Section 6.

3 SIMULATIONS

We have used two sets of simulations, which we call the 'Durham' and 'Seattle' simulations. Both sets contain SPH and DMO simulations of a MW-like galaxy and its immediate environment. They use the volume renormalization or 'zoom-in' technique (Katz & White 1993) to increase computational efficiency, with the mass and spatial resolution of the simulation decreasing with radius from the central galaxy. Each adopts a ΛCDM cosmology; the specific parameters adopted differ slightly with the Seattle (Durham) values being $\Omega_{\rm m} = 0.24$ (0.25), $\Omega_\Lambda = 0.76$ (0.75), $\Omega_{\rm b} = 0.042$ (0.045), $\sigma_8 = 0.77$ (0.9), $n_{\rm s} = 0.96$ (1.0) and in both cases $H_0 = 100\,h\,{\rm km\,s^{-1}\,Mpc^{-1}} = 73\,{\rm km\,s^{-1}\,Mpc^{-1}}$. The setup of the two simulations is broadly comparable but crucial differences appear in the handling of star formation feedback as we will discuss below.

The 'Seattle' galaxy, sometimes known as h258, was first run by Zolotov et al. (2009) and then by Zolotov et al. (2012) at the higher resolution employed in our current work. Its properties have been extensively discussed in the context of the Boylan-Kolchin, Bullock & Kaplinghat (2011) 'too-big-to-fail' problem (Zolotov

et al. 2012); it has also been used as a case study of how baryonic discs can regrow following a major merger at $z = 1$ (Governato et al. 2009). At the end of the simulation, it has built a relatively low-mass MW ($M_{200} = 7.7 \times 10^{11}\,\mathrm{M}_\odot$, where M_{200} is the mass enclosed in a sphere with 200 times the mean cosmic density) with a resolution of $1.3 \times 10^5\,\mathrm{M}_\odot$ (DM) and $2.7 \times 10^4\,\mathrm{M}_\odot$ (gas) and force softening of 170 physical parsecs.

This simulation was run using GASOLINE (Wadsley, Stadel & Quinn 2004), a Tree-SPH code. When hydrodynamics is switched on, it uses a pressure-entropy interpolation kernel to reduce artificial surface tension. Cooling, molecular hydrogen and star formation physics are described in Christensen et al. (2012); feedback is implemented according to the Stinson et al. (2006) blastwave model. Self-bound substructures are identified using Amiga's Halo Finder (Knollmann & Knebe 2009), hereafter AHF, although we processed the final snapshot with SUBFIND (see below) to ensure the same structures are identified by both algorithms.

The Durham simulation is based on an early version of the PM-Tree-SPH code GADGET-3, and takes the same initial conditions as halo Aq-C of the Aquarius suite (Springel et al. 2008). Its highest particle mass resolution (in an $\sim 5\,h^{-1}$ Mpc region around the target halo) is similar to that of the 'level 4' simulation set in Aquarius. The final mass is $M_{200} = 1.8 \times 10^{12}\,\mathrm{M}_\odot$, with a resolution of $2.6 \times 10^5\,\mathrm{M}_\odot$ (DM) and $5.8 \times 10^4\,\mathrm{M}_\odot$ (gas). The force softening is 260 physical parsecs.

Durham baryonic processes are modelled as described in Okamoto et al. (2010), with a number of modifications designed to improve the treatment of SNe-driven winds, which are explained in detail in Parry et al. (2012). Additional details of this simulation are also presented in Okamoto (2013). The central galaxy contains a massive centrifugally supported disc as well as a dispersion-supported spheroid. Self-bound substructures were identified with the SUBFIND algorithm (Springel, Yoshida & White 2001) as modified by Dolag et al. (2009) to take into account the internal energy of gas particles when computing particle binding energies.

The central galaxy in the Durham simulation (of an $\sim 5\,h^{-1}$ Mpc region around the target halo) contains a massive centrifugally supported disc as well as a dispersion-supported spheroid. The final mass of its halo is $M_{200} = 1.8 \times 10^{12}\,\mathrm{M}_\odot$. This simulation was used by Parry et al. (2012) to study the satellite system of an MW-like system. It provided a good match to the average of the satellite luminosity functions of the MW and M31 but formed its brightest satellites in excessively massive haloes, in what became known as the too-big-to-fail problem (Boylan-Kolchin et al. 2011). One of the satellites in this simulation generated a core in its halo as a result of a large inflow of gas into the centre triggered by a triple merger and its subsequent violent expulsion in a starburst.

As described above, there are a number of numerical and physical differences between the two sets of simulations. We will see below that the most important distinction is the type of stellar feedback implemented. In the Durham case, feedback should be seen as 'passive' in the sense of Pontzen & Governato (2014); it produces little or no coupling between the baryonic and DM components of the simulation. Conversely, the Seattle simulations have 'active' feedback that demonstrably couples baryons and DM with energy being passed from the former to the latter (Pontzen & Governato 2012). This means that, for instance, some of the main satellites in the Seattle simulations develop central density cores (Zolotov et al. 2012), which is not generally the case in the Durham simulation, with the exception of the single satellite mentioned above which, in any case, was disrupted shortly after being accreted into the main halo. Thus, when comparing haloes and tagged DM populations in these two sets, we can appreciate the effect of the very different feedback recipes implemented.

3.1 Post-processing

In this paper, we will establish a controlled comparison between the self-consistently formed stars in the simulations described above and 'tagged' stars in DMO runs of the same regions. For full insight, we will also need to study stellar haloes obtained through algorithms intermediate between these two cases. Our series of approaches are similar to those used by Bailin et al. (2014), but differ fundamentally in that they all employ 'live' star formation – associating stellar mass with DM particles in a time-dependent way. They are labelled as follows.

(i) `SPH STARS` – the stellar component of the SPH simulations. These represent an obvious basis from which to assess the success of a tagging scheme, although one should bear in mind that there are a number of differences between SPH and real galaxies; see for instance Stinson et al. (2010); Creasey et al. (2011).

(ii) `SPH TAGGED SF-REAL` – DM particles are tagged within the SPH simulation, and the stellar masses assigned to the particles are calculated using the actual SFRs of the SPH galaxies. Thus, the star particles are not used explicitly but SFRs are guaranteed to match and baryonic effects such as feedback and the presence of a disc can still affect the tagged DM's dynamics.

(iii) `SPH TAGGED SF-MODEL` – as above, DM particles are tagged in the SPH simulation; but SFRs are calculated using an analytic prescription. Specifically, we assume a power-law relation between halo DM mass and SFR. This relation is allowed to vary with redshift, and the power-law indices are obtained by fitting to the SPH SFR as a function of halo mass. Note that C10's tagging scheme actually uses the semi-analytic model GALFORM to obtain SFRs, but in this paper we adopt a simpler prescription to obtain SFRs consistent with, but no longer identical to, those of the SPH comparison simulations.

(iv) `DMO TAGGED SF-MODEL` – particles are tagged in a DMO run of the galaxy. Ultimately, it is the validity of this approach that we wish to investigate, since it resembles most closely the scheme used by C10 to produce observable predictions of halo properties. The SFRs are calculated in the same way as the `SPH TAGGED SF-MODEL` run. Note that again we do not use the C10 model to obtain the SFRs since we wish to test the physics of tagging, not of semi-analytic galaxy formation models.

If tagging fails due to an intrinsic difference in the kinematics of DM and star particles, then this should be clear when comparing the haloes obtained in the `SPH STARS` and `SPH TAGGED SF-REAL`. If, on the other hand, it fails because baryonic effects do affect significantly the assembly of the stellar halo, then the disagreements should arise when comparing the `DMO TAGGED SF-MODEL` to the `SPH STARS` and `SPH TAGGED SF-REAL` runs. Finally, the `SPH TAGGED SF-MODEL` is a control run to check that any disagreements between the SPH and DMO tagging do not in fact occur because the scaling relation used to prescribe the SFRs is too naive.

4 HALO STRUCTURE

The principal aim of particle tagging is to produce tagged stellar haloes with realistic substructures at $z = 0$ (such as stellar streams) and having densities and dynamics comparable to those of real haloes. The purpose of this paper is to investigate some of the

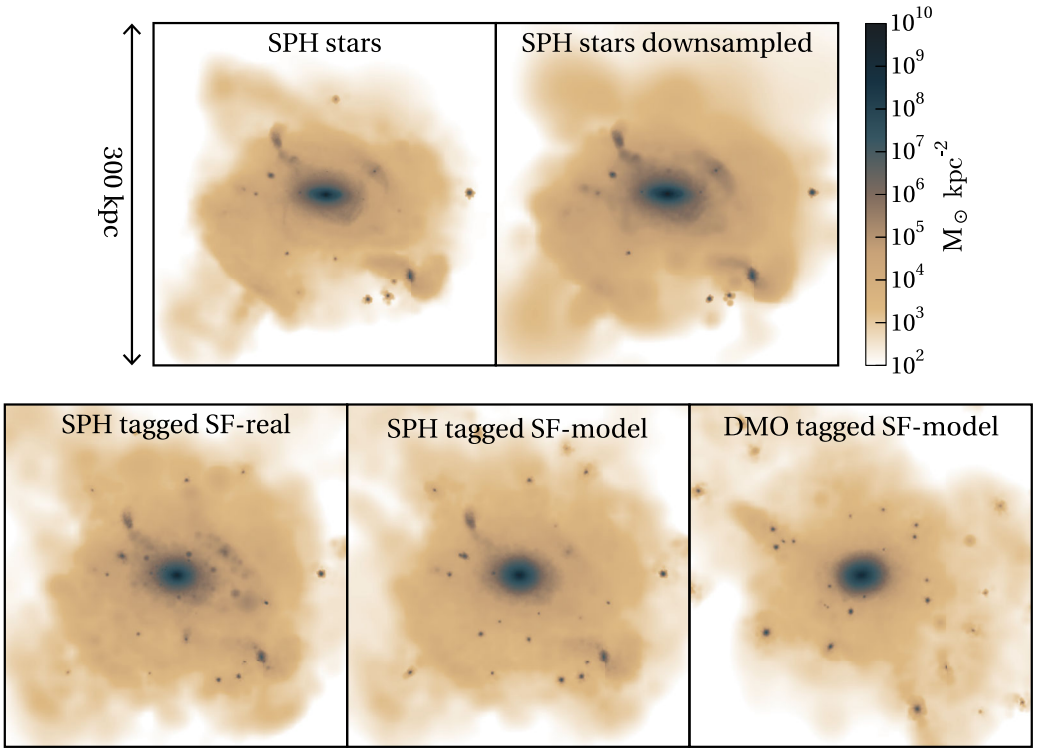

Figure 1. Projected stellar mass surface density at $z = 0$ for SPH stars and the 'particle tagging' outputs for the Seattle simulations. In these panels, tagging is always applied to the top f5 per cent most-bound particles ($f_{\rm mb\,=\,5\,per\,cent}$). Note that a one-to-one correspondence between the DMO tagged and SPH tagged is not expected, as differences between the SPH and DMO runs, such as the presence of baryonic discs in the former, combined with the stochastic nature of halo formation, will make them differ qualitatively (see Section 4).

physics relevant to stellar halo formation rather than to tackle observational matters – this will be left to a companion paper, Cooper et al. (2016) – but we nonetheless need to start with a brief comparison of the observable outputs.

To obtain a qualitative view of how well DM tagging reproduces the features of the SPH stellar halo, we obtained 2D projected density maps of the SPH stars and their tagged DM analogues at $z = 0$, tagging first the DM in the SPH, and then in the DMO simulation (Fig. 1).[1] We find that the `SPH TAGGED` outputs produce a stellar halo containing much the same substructure as the SPH stars; in both cases, stellar streams are clearly discernible, associated with tidally stripped satellites of the main galaxy, and seem to have comparable densities. This suggests that the SPH tagged DM and SPH stars have similar density distributions by the time the simulations reach $z = 0$ – though this does not necessarily imply that the SPH stars and tagged DM were in agreement at the time of tagging. This is an important distinction that will be discussed further in the next section.

The resolution in the tagged DM tends to be lower than in the SPH stars. This is not an intrinsic limitation of particle tagging, but an artefact of the way we carry out the comparison; here, we tag DM in an SPH simulation (and a corresponding DMO simulation), where the mass and spatial resolution in the DM component is lower by a factor of about 10 than those achieved by recent pure *N*-body codes (such as the Aquarius haloes, on which C10 applied their tagging scheme). In order to compare the tagged and SPH star images more fairly, one can thus downsample the latter, taking only every fifth particle (top-right panel of Fig. 1). The effect of this is to decrease the resolution of the streams, which is also observed in the `SPH TAGGED`. In other words, the fact that substructure is somewhat 'blurred' in the tagging images is related to the artificially low resolution.

In fact, the resolution issues become even more subtle and can be seen to be responsible for the visible tendency of tagging to produce larger abundances of subhaloes, even in the `SPH TAGGED SF-REAL` case where the effects of baryonic feedback on SFRs are directly taken into account, and where tidal interactions with the galactic disc still have the ability to disrupt satellite haloes. The number of DM particles tagged is independent of the SFR; therefore, in a halo with low SFR, a large number of particles may be tagged with very small stellar masses. In this situation, the mass resolution locally becomes much higher than that of the SPH stars, which have fixed mass per particle at birth irrespective of SFR. So, although overall the resolution is lower in the tagged halo, we verified that for small subhaloes the resolution is in fact larger in the tagging realizations than in the SPH stars.

There seems to be fairly little qualitative difference between the `SPH TAGGED SF-REAL` and `SPH TAGGED SF-MODEL` runs, which suggests that the simple prescription used for assigning SFRs to DM haloes is adequate for our purposes. In the case of the DMO-tagged simulation, a qualitative comparison is less straightforward, as small differences between the SPH and the DMO simulation runs (as well as the presence of a baryonic disc in the SPH case),

[1] This was carried out with $f_{\rm mb} = 5$ per cent, which produced the best match between SPH stars and tagged DM: we emphasize, however, that the particular values of $f_{\rm mb}$ used in this paper are meant purely to illustrate the differences between tagging and SPH, and not to reproduce observable quantities in the Local Universe.

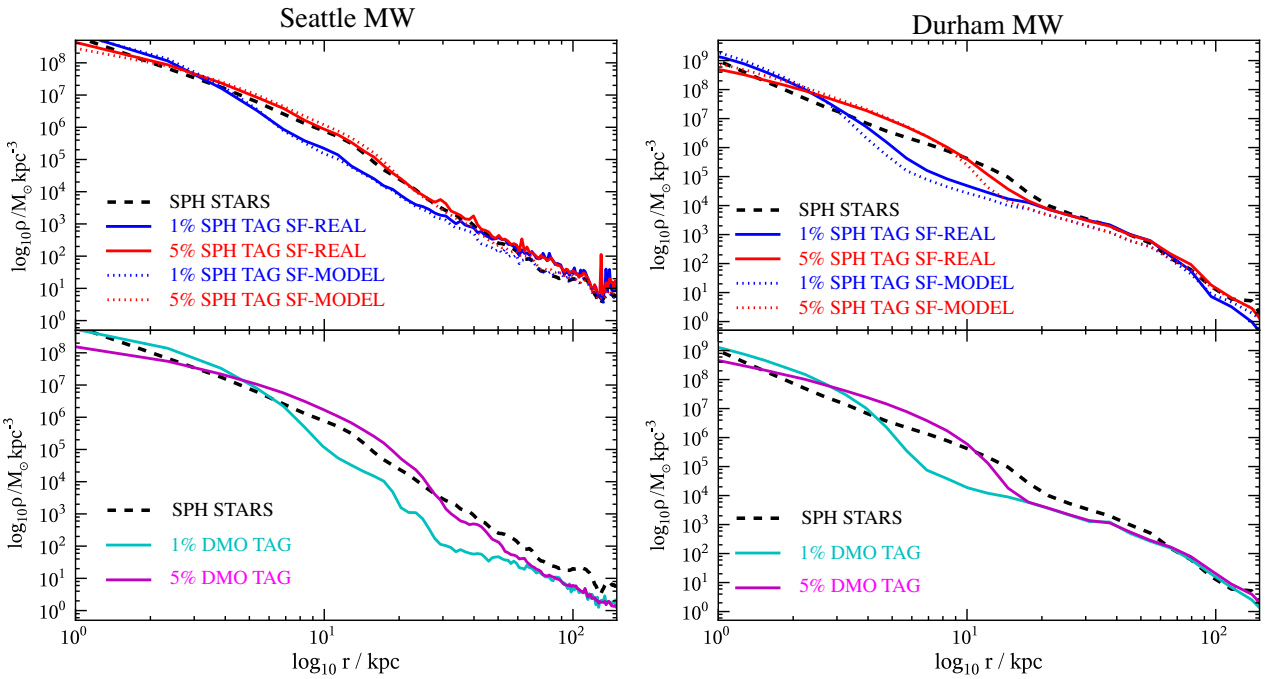

Figure 2. Spherically averaged density profile of the main halo, excluding self-bound substructures, for the SPH stars and tagged DM, for most-bound fractions ($f_{\rm mb}$s) of 1 and 5 per cent, in the Seattle (left-hand panel) and Durham (right-hand panel) simulations. The 5 per cent cases produce output densities within a factor of a few of the SPH results over seven orders of magnitude in stellar density in all cases.

combined with the stochastic nature of halo structure formation,[2] mean that even the locations of DM substructures are quite different. Although streams and substructures are present, they do not correspond directly to the SPH streams, and there seem to be a significantly larger number of subhaloes than in the SPH case. We will argue below that this last difference may, at least in some cases, be an effect of the 'bursty' feedback implemented in the Seattle simulations, where some satellites develop DM cores in their inner regions, and thus become more susceptible to tidal disruption when passing through the galactic disc – see Zolotov et al. (2012), Brooks & Zolotov (2014) and also Peñarrubia et al. (2010).

For a more quantitative comparison between the SPH stars and tagged haloes, we turn to spherically averaged density profiles for the main halo and a few satellite galaxies. Fig. 2 shows the main stellar halo density for various tagging realizations for the SPH and DMO cases (top and bottom panels) in the Seattle and Durham simulations (left and right). In each panel, the thick black dashed line shows the `SPH STARS`. For all three tagging realizations, taking $f_{\rm mb} = 5$ per cent produces output densities within a factor of a few of the SPH results over seven orders of magnitude in stellar density. Notably, the Seattle `SPH TAGGED` cases are in particularly good agreement – this result can be tied to strong active star formation feedback and will be discussed further below and in Section 5.

Conversely, the worst agreement arises with `DMO` tagging within the inner few kpc of the main galaxy. Tagging will be a poor description of the star distribution in regions where baryons dominate, i.e. near the disc and bulge of the main galaxy. The inaccuracies can then propagate outwards if a significant fraction of the halo stars were originally disc stars that were scattered out to the stellar halo. A more detailed discussion of this process and its importance in Seattle simulations can be found in Zolotov et al. (2009).

We also obtained density profiles for the main satellites (Fig. 3). In reading order, the figure shows the first to third most massive satellite in the Seattle simulations, then the most massive of the Durham satellites. Once again the SPH stars are shown by the thick dashed line – one can read off that the agreement between the SPH stars and tagging $f_{\rm mb} = 5$ per cent in both SPH and DMO is broadly quite good. However, the most massive Seattle satellite (top-left panel) shows a striking discrepancy between the `DMO` and `SPH` cases. It has previously been shown for the Seattle simulations that the SN feedback causes the dynamics of the DM and baryonic component to couple strongly, creating DM density cores (Pontzen & Governato 2012) in the central regions. Tagged and 'real' star particles alike will be thrown to larger radii by this process. But in the DMO simulation, the process is of course missing – so the `DMO TAGGED` cases form stellar components with significantly too short a scalelength. This begins to show that the agreement between tagging and SPH will depend on what kind of feedback recipe is used in the SPH (i.e. 'active' vs. 'passive').

In fact, this deep connection between the mode of stellar feedback and the behaviour of tagging algorithms can be further reinforced by studying the difference between the different tagging fractions ($f_{\rm mb} = 1$ or 5 per cent, hereafter 'tag 1' and 'tag 5'). As we commented briefly above, in the Seattle `SPH TAGGED` outputs setting 1 or 5 per cent seems to make surprisingly little difference to the final density profiles of the halo, especially in the satellites, or in the main galaxy in the outer regions, at $r \geq 20$–30 kpc – which is the region where we expect tagging to produce a reasonably accurate description of the halo. Increasing the number of tagged particles by a factor of 5 does not for instance change the scalelength of the

[2] Substructure in the galactic halo reflects the hierarchical build-up of galaxies in ΛCDM: because this process is highly non-linear, small initial differences in the halo progenitors in the DMO and SPH runs, for instance due to the absence or presence of baryonic potentials, are amplified over the course of the cosmological simulation, resulting in the build-up of substructure that looks qualitatively different in the DMO and SPH runs.

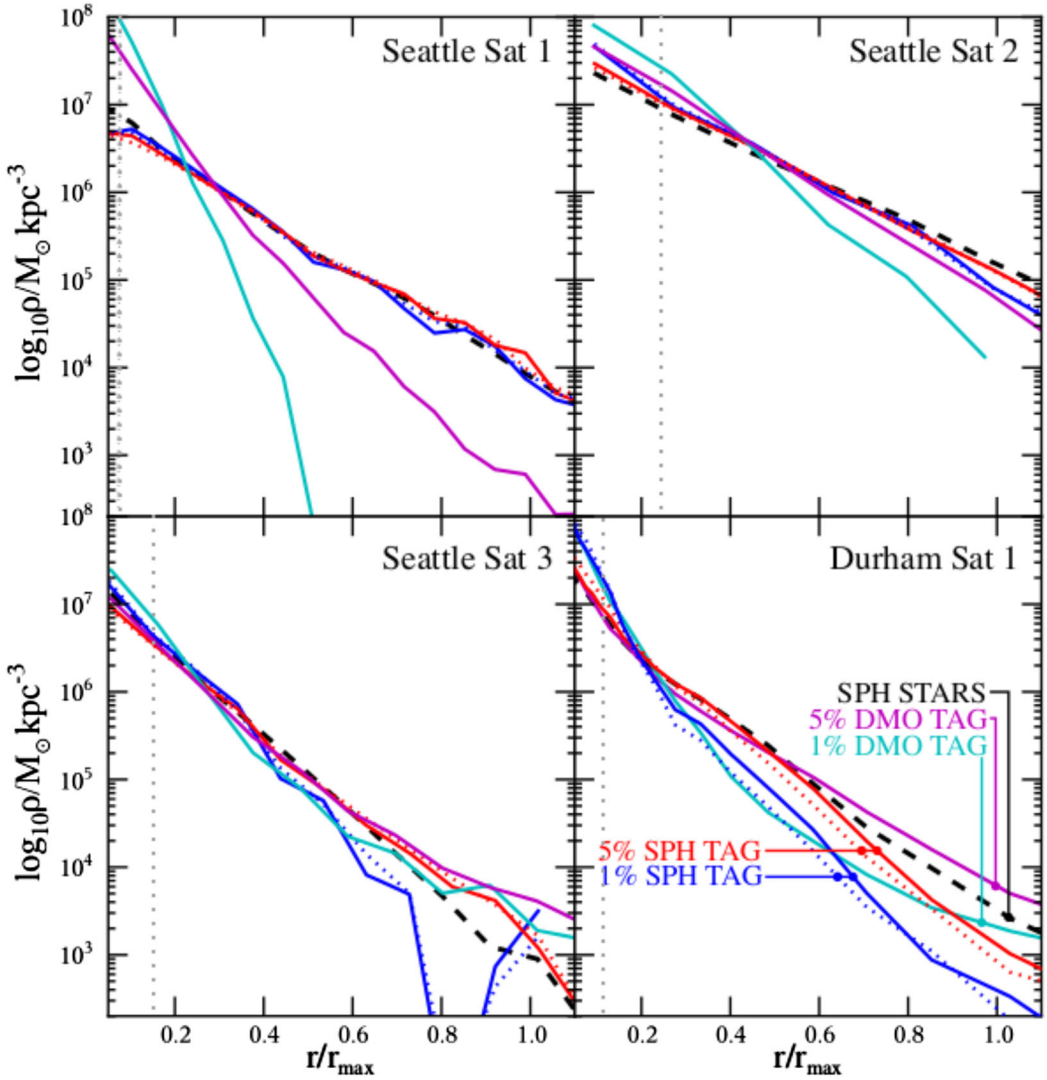

Figure 3. Spherically averaged density profiles of the four most massive satellites for the SPH stars and the different tagging realizations. Densities are normalized so that the total tagged mass equals the SPH stellar mass. Radii are normalized to $r_{\rm max}$, the radius at which the circular velocity achieves its maximum value. The bottom-right panel shows the profile of the largest satellite in the Durham simulations. All other satellites come from the Seattle simulations. For Seattle Satellite 1, the scalelengths are significantly underestimated in all DMO cases because the feedback coupling – that causes collisionless particles including stars to migrate outwards – is missing. In other cases, reasonable agreement can be achieved using 5 per cent tagging. Satellite stellar (dark) particle numbers are $3.7 \times 10^4 (8.5 \times 10^4)$, $8.0 \times 10^3 (1.4 \times 10^4)$, $3.5 \times 10^3 (9.9 \times 10^3)$, $9.2 \times 10^3 (5.4 \times 10^5)$ $\mathrm{M}_\odot$ for Seattle Sat 1, 2, 3 and Durham Sat 1, respectively. The vertical grey dotted line indicates the location of 3 × softening.

exponential density profiles, or their general shape (the discrepancy between `SPH STARS` and `SPH TAGGED` 1 per cent in the smallest Seattle satellite, Sat 3, at $r/r_{\rm max} \geq .7$ is Poisson noise due to the fairly small number of particles tagged in these regions). This suggests that the overall density profiles are primarily being set by dynamical processes *after tagging*, not by the details of the tagging itself. The expected increased prominence of these processes when feedback is active is reflected in near-complete insensitivity to $f_{\rm mb}$ in the Seattle `SPH TAGGED` cases.

The Durham simulations have a more passive type of feedback and are therefore missing the dynamic redistribution of stars that we see in the Seattle cases. The bottom-right panel of Fig. 3 shows the profile of the largest satellite in the Durham simulations: agreement between the tagging realizations and the SPH stars is not as good as for the Seattle satellites. Moreover, the SPH tag 1 and tag 5 runs do not resemble one another as closely as they do in the Seattle satellites. This is suggestive, but we now turn to a more explicit way to verify that diffusion of stars through the energy space is a significant effect.

5 ENERGY DIFFUSION

In the previous section, we compared the stellar haloes from our various tagging schemes and found, from a number of perspectives, agreement between apparently very different approaches. We have suggested that these can be tied to dynamical redistribution of the stars after they have been formed; we will now provide a direct analysis to support that claim.

We first trace the evolution of the radial scalelength of a population of tagged particles over a period of a few Gyr after its initial assignment, as follows. In an early simulation snapshot ($z = 8$), we select the most-bound 1 and 5 per cent of DM particles, as well

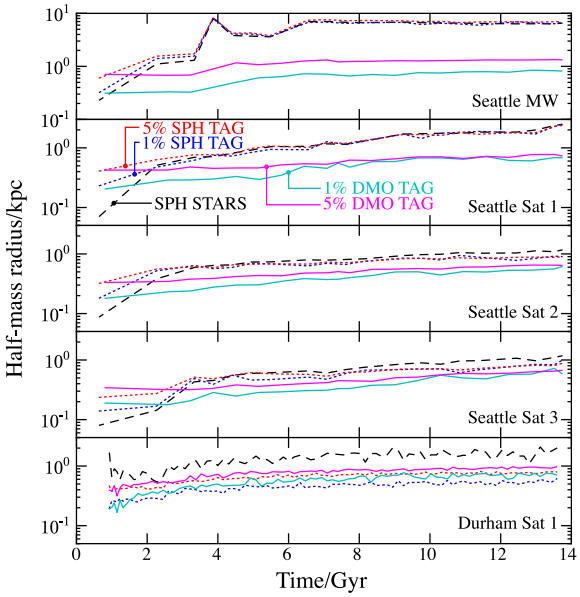

Figure 4. Evolution of the half-mass radius of different tagged populations and the stars they are meant to represent in the Seattle main galaxy (top panel) and its three largest satellites (next three panels, in order of satellite size). The lowest panel shows Durham satellite 1. The colour scheme is as for the density profiles: black for the SPH stars, blue and red for the SPH tagged 1 and tagged 5, respectively, and cyan and magenta for the DMO tagged 1 and tagged 5, respectively. In all cases, the half-mass radius at early times is sensitive to the tagging mode, but at late times this dependence is substantially reduced. This is tied to diffusion of particle energies as described in the text, and is a particularly strong effect when 'active' feedback is present as in the Seattle SPH simulations.

as the recently formed stars. We then obtain the radius enclosing half of the total mass of these particles. We track these same particles over time, calculating their half-mass radius at each snapshot. The results are shown in Fig. 4 for (top to bottom panels) the major progenitor and the three most massive satellites in the Seattle simulations, followed by the most massive satellite in the Durham simulations. In the appendix, we reproduce this result for Seattle satellite 1 starting with a later snapshot ($z = 1$), to check that the behaviour observed is generic.

At the tagging snapshot, $z = 8$ (far left of each panel), the half-mass radii do not typically match those of the stars, with initial discrepancies between `SPH TAGGED SF-MODEL` (dotted lines), `DM TAGGED SF-MODEL` (solid lines) and `SPH STARS` (dashed line) reaching an order of magnitude. The difference between tagging the 1 or 5 percent most-bound DM particles in the haloes is also clearly discernible: as naively expected, when a larger number (by a factor of 5) of particles are tagged, their distribution is more diffuse, and the half-mass radius is larger.

However, as we follow the evolution of this distribution, all populations 'diffuse'[3] outwards to larger radii; initially, compact populations tend to diffuse faster and so the initial differences in scale radii are significantly eroded. Particularly in the Seattle cases, the tagged particles of the `SPH` runs (dotted lines) tend to converge to mimic the stars (dashed line) – irrespective of the binding energies at which they were originally selected. In these cases, the convergence between the half-mass radii of the tag 1, tag 5 and stars occurs on a time-scale of around 3 Gyr, and these three initially distinct populations become virtually indistinguishable.

In the DMO tagged assignments (solid lines) convergence is slower, but still significant. In Seattle satellites 2 and 3, for example, the half-mass radius discrepancy narrows from an initial discrepancy of a factor 2 at $z = 8$ to agreement by $z = 0$. However, unlike the SPH case, it takes the entire Hubble time for this to occur and in the case of satellite 2 it does not even run to completion. Furthermore in the central galaxy, the diffusion process ceases after a major merger at a time of around 4 Gyr. This is consistent with a picture of diffusion being driven primarily by time-dependence in the potential of a spheroidal halo – after this time the galaxy is quiescent and, in the case of the SPH run, has developed a stable disc structure.

For each satellite, the diffusion is faster and more sustained in the SPH case than in the DMO case. This follows because baryonic feedback enhances the process by producing more stochastic time-dependence in the potential, particularly in the case of satellite 1 (second panel from top in Fig. 4) where the populations from the SPH simulation continue migrating outwards throughout cosmic time. As discussed in Section 4, this satellite produces a feedback-driven DM density core in the hydrodynamic cases. The outward migration is a symptom of this process and by definition is not present in the DMO cases.

With the above in mind, we can start to see the diffusion process as a double-edged sword. On the one hand, it does tend to drive tagging realizations into better agreement, because it reduces sensitivity to the initial choice of which particles to tag. On the other, the strength of the diffusion can be enhanced by baryonic processes leading to a new, fundamental source of discrepancy with DMO simulations. In the Durham cases (illustrated here by Satellite 1, the lowest panel of Fig. 4), the DMO and SPH cases are in much better agreement, but the convergence is also much weaker. Both these aspects follow from the relatively passive approach to feedback taken.

In practice, this means that – if one believes in the kind of bursty star formation histories that lead to the 'active' feedback coupling – DMO tagging schemes will need to tag particles that are less bound than the regions in which star formation actually takes place, because they miss processes that kick stars up to higher energies. Concretely, the lower left panel of Fig. 2 shows 5 per cent tagging in the Seattle DMO simulations produce better fits to the SPH star density profiles than 1 per cent tagging – and yet Fig. 4 shows directly that at the time of formation, the SPH STARS are more tightly bound even than the 1 per cent case.

5.1 Energy and angular momentum

We can obtain another view of the importance of diffusion by studying the process in energy space. First, we obtain the energy distributions of recently formed stars and their tagged DM analogues (using different values of $f_{\rm mb}$) at the time the DM is assigned a stellar mass, and track the evolution of these distributions (for the same set of particles) over a few gigayears. We confirm that, at the time of tagging, the recent stars and most-bound DM particles do have very different energies (top panels, Fig. 5; the three panels from left to right show Seattle MW, Satellite 1 and Durham Satellite 1).

One can now see explicitly how in the Seattle SPH cases, the baryonic feedback drives the full `SPH STARS` and `SPH TAG MODEL-SF` energy distributions into agreement, irrespective of the starting $f_{\rm mb}$. Once again the DMO cases do evolve to reduce initially stark differences in the energy distributions, but this diffusion is not

[3] This diffusion is still collisionless, driven by time-dependence in the potential and collective effects rather than two-body encounters.

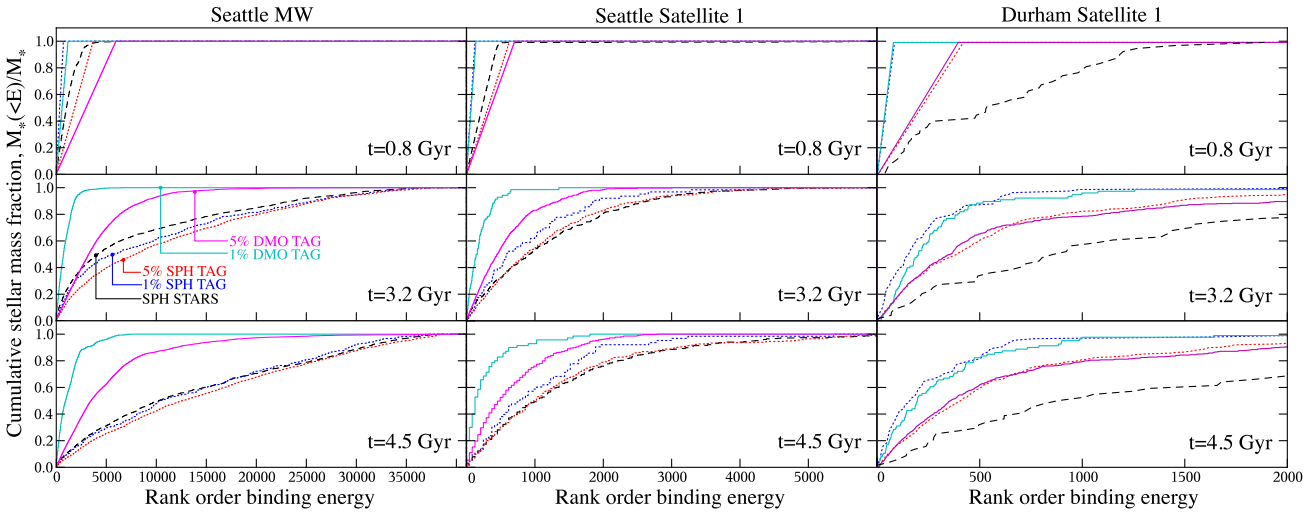

Figure 5. Diffusion in the rank binding energy distribution of recently formed stars and their analogue tagged DM in the Seattle main halo (left-hand panel) and largest satellite (middle panel), as well as the Durham largest satellite (right-hand panel). From top to bottom, the panels represent the simulations at simulation output times: $t = 800$ Myr, 3200, 4500, where the stars are those formed at $t = 800$ Myr, and the DM has been assigned a stellar mass at the same time. The evolution over time is characterized by a drift to larger scale radii, and (in most cases) towards closer agreement between initially distinct populations. As also seen in Figure 4, the effect is strongest in the Seattle SPH cases where active feedback generates strong potential fluctuations.

complete and the energy distributions of this population of stars are significantly different from those of the SPH case.

Comparing satellite 1 from the Seattle and Durham SPH simulations (middle and right-hand panel, respectively), one can see explicitly how the difference between active and passive feedback is crucial. In the Durham case, the differences in the diffusion between SPH and DMO are much less marked because the gas evolution has relatively little impact on the collisionless dynamics. Once again, we see the dual impact of diffusion – it substantially reduces sensitivity to the initial distribution of star formation events, but the extent of diffusion depends on the nature of feedback.

Finally, we verified that a very similar view can be obtained in angular momentum space (Fig. 6) – the chaos associated with potential fluctuations from mergers or stellar feedback causes the distributions to drift away from their initial arbitrary shapes. The non-conservation of angular momentum is not what is surprising about this picture (in aspherical systems, angular momentum is not expected to be conserved), but the fact that an initial arbitrary sample of particles will drift towards the same distribution in angular momentum space, so that the system exhibits 'spherical ergodicity' in the sense of Pontzen et al. (2015). Although diffusion in both angular momentum and energy is only explicitly studied here at $z = 8$, it in fact occurs up to the point when stars form in a stable disc, which is after most of the halo stars have formed (a more detailed discussion of this is provided in the appendix).

In conclusion, there is very strong evidence for the diffusion of orbits through energy and angular momentum space being a crucial ingredient in deciding the final distribution of stars in spheroidal systems. This in turn has significant implications for interpreting the existing literature and for future schemes attempting particle tagging, as we now discuss.

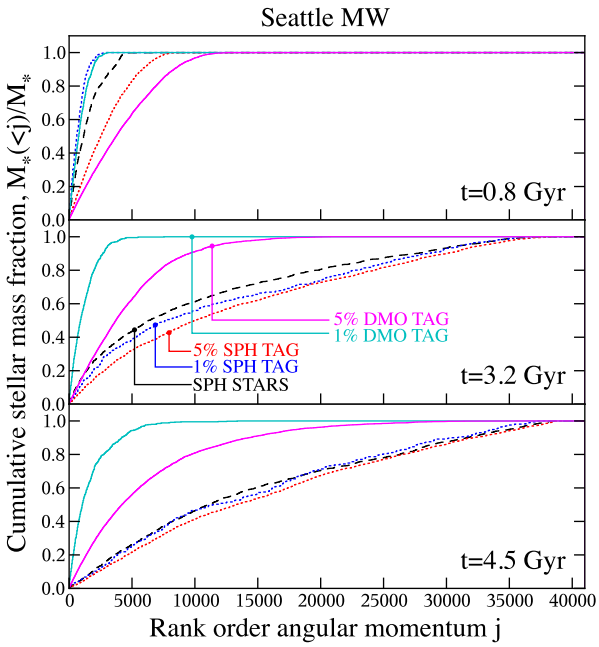

Figure 6. The angular momentum distribution of a population of stars and their analogue tagged DM in the main halo, selected at high redshift ($z = 8$) in the Seattle simulations. Stars like these that end up in the halo, rather than the disc, have distributions of angular momentum that evolve rapidly – similar to how their energy distribution changes (Fig. 5). Stars forming later and contributing to the disc in the SPH case retain their angular momentum.

6 DISCUSSION AND CONCLUSIONS

We have re-implemented and investigated a particle tagging scheme for simulating stellar haloes in DMO simulations, first used and described in C10. The scheme assigns a 'stellar mass' to the most-bound DM particles in each halo at every simulation output time. In our case, we use this method to establish a comparison similar in spirit to that of Bailin et al. (2014), constructing a series of different stellar haloes that increasingly differ from the SPH stars. Our focus is on understanding the physics that sets the distribution of stars within each subhalo, and hence in the stellar halo of an MW-like galaxy.

Our main conclusions are as follows.

(i) Tagging a fixed fraction of DM within SPH simulations reproduces qualitative features of the SPH stellar halo structure and substructure (Fig. 1); tagged stellar haloes have density profiles very similar to the SPH haloes (compare red and blue 'tagged' lines to the black dashed line in Fig. 2).

(ii) Performing the same experiment in the DMO run produces more pronounced differences between the tagged halo and reference SPH stars halo, although for 5 per cent tagging one obtains similar scalelengths and density profiles that deviate from the SPH stars by less than 1 dex (see Fig. 3). The exception to this pattern is Seattle's satellite 1, which has a large DM core in the SPH run; therefore, by definition, collisionless particles in the DMO run end up on the 'wrong' orbits relative to the SPH case.

(iii) All the above results can be tied to diffusion of the tagged DM particles through energy space. Populations that are tagged in differing regions nonetheless end up with similar phase space distributions if sufficient time is given between the initial assignment and the point at which the stellar halo properties (densities, satellite profiles and so on) are measured (e.g. Figs 4, 5 and A2).

(iv) The agreement between tagging and SPH is affected by the type of SN feedback recipes implemented in the SPH subgrid physics. The Seattle simulations have a strong, 'bursty' feedback recipe (Stinson et al. 2006). We have already commented on the core in satellite 1, but even elsewhere in the Seattle simulations we see considerably accelerated diffusion compared to the DMO runs (e.g. Fig. 5). Conversely, the Durham simulations (which have 'passive' feedback, rather than Seattle's 'active' feedback; Pontzen & Governato 2014) drive the diffusion at rates much more similar to the DMO case.

Another way to phrase our conclusions is that (in a spheroidal, pressure-supported structure) once a star has formed, the collisionless dynamics will make initially different energy and angular momentum distributions of the tagged and star particles converge. Future work on stellar tagging needs to take this into account. A key recommendation is that, when using fixed fraction schemes such as that of C10, one should consider tagging DM in regions considerably larger than the strict star formation region of a halo, to make up for missing energy kicks that might arise from astrophysics in the real Universe.

On the other hand, the success of schemes that tag the DM particles just prior to satellite infall should therefore rely more on a correct estimate of where the stars 'end up' in phase space relative to the DM at the time of infall; Libeskind et al. (2011), for instance, define a threshold value of the potential in each halo, above which DM particles are used as proxy for stars. This threshold is optimized for each individual halo, so that the radial distribution of tagged DM after infall resembles that of SPH stars as closely as possible. In this scheme, good agreement between SPH and tagging can also be reached, but should depend more sensitively on the value of the threshold adopted, since this implicitly contains the dynamical information ('how diffusion eventually redistributes stellar orbits') that the C10 scheme follows explicitly. We note, however, that the details of the agreement between SPH and tagging (especially in the surviving satellite profiles) will also depend, to a considerable extent, on the type of feedback prescription used, as well as the specific halo histories. In this study, we have focused on elucidating some of the physical processes that can drive 'tagging' and SPH schemes into better or worse agreement, and establish a more detailed comparison between the results of different DM painting methods in a companion paper (Cooper et al. 2016).

Diffusion itself may be driven in the DMO simulation by mergers or tidal interactions (Kandrup, Vass & Sideris 2003; Stickley & Canalizo 2012) and accelerated in the SPH simulation by baryonic processes such as interaction with a disc or SN feedback (Valluri et al. 2013). Further study of these processes will be necessary to understand more fully the exact domain of applicability of particle tagging.

Other proposals for improving and understanding tagging were given by Bailin et al. (2014) and focus on selecting a more appropriate region of the phase space, in particular by considering angular momentum. Our work suggests that, in a spheroidal system, differences in initial angular momentum get smoothed out in much the same way as the differences in energy. Therefore selecting the 'correct' particles to tag is as much about studying dynamical evolution as it is about characterizing the orbits of recently formed stars.

ACKNOWLEDGEMENTS

We wish to thank our anonymous referee for helpful comments, as well as James Binney for stimulating discussion. TLB acknowledges an ERC studentship. AP is supported by a Royal Society University Research Fellowship. APC is supported by a COFUND/Durham Junior Research Fellowship under EU grant agreement 267209. FG was funded by NSF grants AST-0908499, AST-0607819 and NASA 13-ATP13-0020. CSF acknowledges ERC Advanced Investigator Grant COSMIWAY and support from Science and Technology Facilities Council grant ST/F001166/1,ST/L00075X/1. FG was funded by NSF grants AST-0908499, AST-0607819 and NASA 13-ATP13-0020. OHP was supported by NASA grant NNX10AH10G and by NSF grant CMMI1125285. We made use of PYNBODY *N*-body analysis software (Pontzen et al. 2013) in our analysis for this paper (https://github.com/pynbody/pynbody). This research used the DiRAC Facility, jointly funded by STFC and the Large Facilities Capital Fund of BIS. The Seattle simulations were run at NASA HEC.

REFERENCES

Abadi M. G., Navarro J. F., Steinmetz M., 2006, MNRAS, 365, 747
Bailin J., Bell E. F., Valluri M., Stinson G. S., Debattista V. P., Couchman H. M. P., Wadsley J., 2014, ApJ, 783, 95
Baugh C. M., 2006, Rep. Prog. Phys., 69, 3101
Bell E. F. et al., 2008, ApJ, 680, 295
Boylan-Kolchin M., Bullock J. S., Kaplinghat M., 2011, MNRAS, 415, L40
Brooks A. M., Zolotov A., 2014, ApJ, 786, 87
Bullock J. S., Johnston K. V., 2005, ApJ, 635, 931
Christensen C., Quinn T., Governato F., Stilp A., Shen S., Wadsley J., 2012, MNRAS, 425, 3058
Cole S., Lacey C. G., Baugh C. M., Frenk C. S., 2000, MNRAS, 319, 168
Cooper A. P. et al., 2010, MNRAS, 406, 744
Cooper A. P., Cole S., Frenk C. S., Helmi A., 2011, MNRAS, 417, 2206
Cooper A. P., D'Souza R., Kauffmann G., Wang J., Boylan-Kolchin M., Guo Q., Frenk C. S., White S. D. M., 2013, MNRAS, 434, 3348
Cooper A. P., Cole S., Frenk C. S., Le Bret T., Pontzen A., 2016, preprint (arXiv:astro-ph/1611.03497)
Creasey P., Theuns T., Bower R. G., Lacey C. G., 2011, MNRAS, 415, 3706
De Lucia G., Helmi A., 2008, MNRAS, 391, 14
Dolag K., Borgani S., Murante G., Springel V., 2009, MNRAS, 399, 497
Eggen O. J., Lynden-Bell D., Sandage A. R., 1962, ApJ, 136, 748
Font A. S., McCarthy I. G., Crain R. A., Theuns T., Schaye J., Wiersma R. P. C., Dalla Vecchia C., 2011, MNRAS, 416, 2802
Frenk C. S., White S. D. M., Efstathiou G., Davis M., 1985, Nature, 317, 595

Gómez F. A., Helmi A., Cooper A. P., Frenk C. S., Navarro J. F., White S. D. M., 2013, MNRAS, 436, 3602
Governato F. et al., 2009, MNRAS, 398, 312
Helmi A., White S. D. M., 1999, MNRAS, 307, 495
Helmi A., White S. D. M., de Zeeuw P. T., Zhao H., 1999, Nature, 402, 53
Helmi A., Cooper A. P., White S. D. M., Cole S., Frenk C. S., Navarro J. F., 2011, ApJ, 733, L7
Kandrup H. E., Vass I. M., Sideris I. V., 2003, MNRAS, 341, 927
Katz N., White S. D. M., 1993, ApJ, 412, 455
Kauffmann G., White S. D. M., Guiderdoni B., 1993, MNRAS, 264, 201
Knollmann S. R., Knebe A., 2009, ApJS, 182, 608
Laporte C. F. P., Walker M. G., Peñarrubia J., 2013, MNRAS, 433, L54
Libeskind N. I., Knebe A., Hoffman Y., Gottlöber S., Yepes G., 2011, MNRAS, 418, 336
Maxwell A. J., Wadsley J., Couchman H. M. P., Mashchenko S., 2012, ApJ, 755, L35
Navarro J. F., Eke V. R., Frenk C. S., 1996, MNRAS, 283, L72
Okamoto T., 2013, MNRAS, 428, 718
Okamoto T., Frenk C. S., Jenkins A., Theuns T., 2010, MNRAS, 406, 208
Parry O. H., Eke V. R., Frenk C. S., Okamoto T., 2012, MNRAS, 419, 3304
Peñarrubia J., Benson A. J., Walker M. G., Gilmore G., McConnachie A. W., Mayer L., 2010, MNRAS, 406, 1290
Pontzen A., Governato F., 2012, MNRAS, 421, 3464
Pontzen A., Governato F., 2014, Nature, 506, 171
Pontzen A., Roškar R., Stinson G. S., Woods R., Reed D. M., Coles J., Quinn T. R., 2013, Astrophysics Source Code Library, record ascl:1305.002
Pontzen A., Read J. I., Teyssier R., Governato F., Gualandris A., Roth N., Devriendt J., 2015, MNRAS, 451, 1366
Rashkov V., Madau P., Kuhlen M., Diemand J., 2012, ApJ, 745, 142
Read J. I., Gilmore G., 2005, MNRAS, 356, 107
Searle L., Zinn R., 1978, ApJ, 225, 357
Springel V., Yoshida N., White S. D. M., 2001, New Astron., 6, 79
Springel V. et al., 2008, MNRAS, 391, 1685
Stickley N. R., Canalizo G., 2012, ApJ, 747, 33
Stinson G., Seth A., Katz N., Wadsley J., Governato F., Quinn T., 2006, MNRAS, 373, 1074
Stinson G. S., Bailin J., Couchman H., Wadsley J., Shen S., Nickerson S., Brook C., Quinn T., 2010, MNRAS, 408, 812
Tissera P. B., Scannapieco C., Beers T. C., Carollo D., 2013, MNRAS, 432, 3391
Valluri M., Debattista V. P., Stinson G. S., Bailin J., Quinn T. R., Couchman H. M. P., Wadsley J., 2013, ApJ, 767, 93
Wadsley J. W., Stadel J., Quinn T., 2004, New Astron., 9, 137
White S. D. M., Frenk C. S., 1991, ApJ, 379, 52
White S. D. M., Rees M. J., 1978, MNRAS, 183, 341
Zolotov A., Willman B., Brooks A. M., Governato F., Brook C. B., Hogg D. W., Quinn T., Stinson G., 2009, ApJ, 702, 1058
Zolotov A., Willman B., Brooks A. M., Governato F., Hogg D. W., Shen S., Wadsley J., 2010, ApJ, 721, 738
Zolotov A. et al., 2012, ApJ, 761, 71

APPENDIX A: IS DIFFUSION GENERIC BEHAVIOUR FOR HALO STARS?

In this appendix, we present some tests of the robustness of our conclusions regarding the importance of diffusion.

In the main text, we argued that diffusion processes could drive the dynamics of tagged DM particles to converge towards those of the SPH stars, and illustrated this behaviour by showing how the distribution in binding energies and angular momenta of SPH stars and tagged particles become similar over a few snapshots (e.g. Figs 5, 6). Here, we discuss whether the diffusion observed in these snapshots is generic, and whether most halo stars are likely to have been affected. Indeed, most examples of diffusion given in the main body of the text (e.g. Fig. 5) focus on stars tagged at fairly high redshift ($z = 8$), so the question was, first, to investigate whether most halo stars did form at early times, and secondly, to check whether diffusion was likely to occur when these stars formed. Fig. A1 displays the formation history of stars located in the Seattle simulation's main galaxy's stellar halo at $z = 0$. Most of the stars in the final halo formed at redshifts between 8 and 1. We then

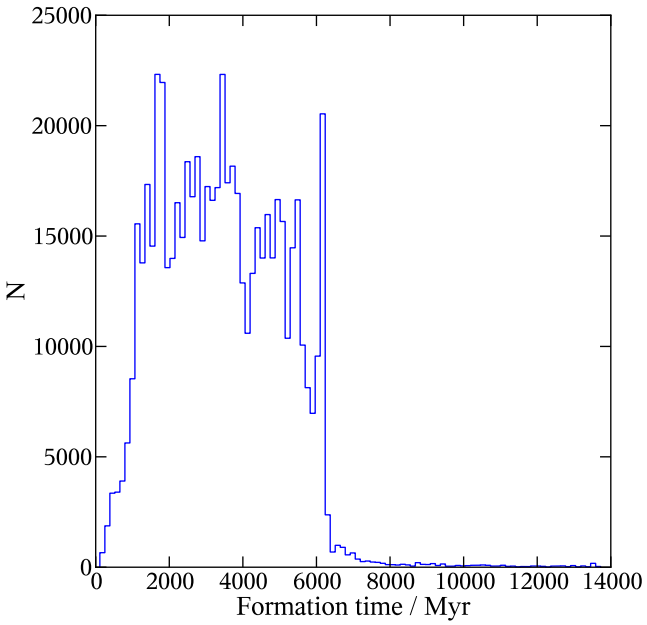

Figure A1. Formation history of halo stars. These are stars that lie in the central galaxy's stellar halo at $z = 0$: most of these formed at early times, in satellite haloes that were later accreted.

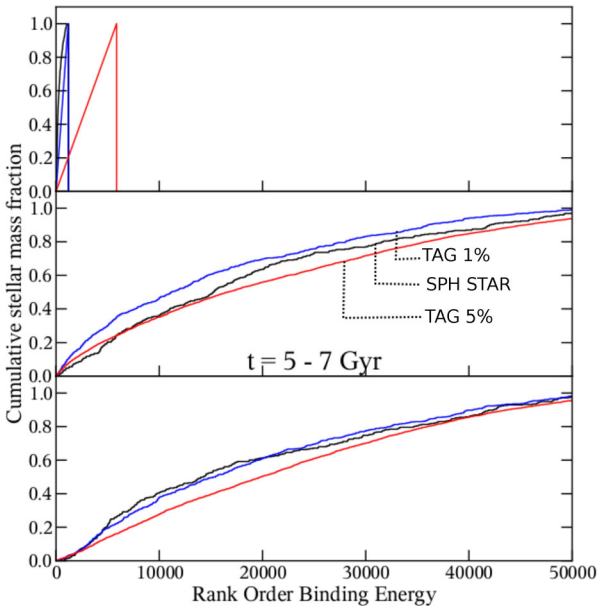

Figure A2. Diffusion in the rank binding energy of recently formed stars and their tagged DM analogues in the Seattle SPH simulations (same as Fig. 5 for Seattle Satellite 1, but at later times and for SPH only). Distributions in binding energy at $t = 5$, 6 and 7 Gyr (in the upper, middle and bottom panels, respectively) of recent stars (black line), DM particles tagged in the SPH with most-bound fractions of 1 and 5 per cent (blue and red lines, respectively).

confirmed that diffusion remains important up to $z = 1$ by following the evolution in binding energy of stars and DM particles tagged at this time in the largest satellite of the Seattle SPH simulations (Fig. A2). In general, we found that diffusion tended to become far less important at later times, especially in the main galaxy where the presence of a stable, rotationally supported disc prevented stars and tagged particles from diffusing in energy and angular momentum space: although we have not here investigated in detail the exact physical mechanisms driving diffusion, this does suggest that out-of-equilibrium processes like 'violent relaxation', perhaps enhanced by high SFRs and/or frequent minor mergers at early times, may be important. Thus, diffusion does in fact occur mostly between $z = 8$ and 1, its importance decreasing starkly afterwards as haloes become more stable; but, because this is also the period where most stellar halo stars formed, diffusion processes will be important in shaping their dynamical history and thus their final distribution in the halo at $z = 0$, as argued in the main body of the text.

This paper has been typeset from a TEX/LATEX file prepared by the author.